Journal of the Meteorological Society of Japan, Vol. 90, No. 5, pp. 673−684, 2012
DOI: 10.2151/jmsj.2012-507

NOTES AND CORRESPONDENCE

El Niño Modoki and the Summer Precipitation Variability over South Korea: A Diagnostic Study

Jong-Suk KIM, Wen ZHOU

School of Energy and Environment, City University of Hong Kong, Hong Kong, China
Guy Carpenter Asia-Pacific Climate Impact Center, City University of Hong Kong, Hong Kong, China

Xin WANG

School of Energy and Environment, City University of Hong Kong, Hong Kong, China

and

Shaleen JAIN

Department of Civil and Environmental Engineering, University of Maine, Orono, Maine, USA
Climate Change Institute, University of Maine, Orono, Maine, USA

(Manuscript received 5 March 2012, in final form 24 June 2012)

Abstract

Recent studies that characterize central tropical Pacific warming (often referred to as El Niño Modoki) and its teleconnections to East Asia show coherent teleconnection patterns during boreal summer. Observed increases in the frequency of El Niño Modoki and a lack of understanding regarding its impacts on precipitation over the Korean peninsula motivate our work. In this study, we investigate the regional precipitation patterns over South Korea associated with El Niño and El Niño Modoki events during the June-September season. The results show significant and consistent increases in the seasonal precipitation totals and maximum precipitation, as well as extreme rainy days during the decay of El Niño Modoki. In contrast, there is a reduction of moisture fluxes into South Korea in the case of the eastern Pacific El Niño. The analysis presented here provides an improved understanding of the potential impacts of the tropical Pacific sea surface temperature on warm-season (June-September) water availability and hydrometeorological extremes over the Korean peninsula.

1. Introduction

In recent years, numerous studies have sought to characterize the spatial temporal variations and change in the tropical Pacific sea surface temperatures. In particular, the changing character of El Niño-Southern Oscillation (ENSO) and its remote impacts posit significant challenge for regional impacts and adaptation. Of particular interest in this regard is the empirical characterization of the El Niño Modoki (Ashok et al. 2007; Weng et al. 2007), having a characteristic pattern that is concentrated in the central equatorial Pacific. Weng et al. (2007) used three strongest El Niño and El Niño Modoki events to identify the possible impacts

Corresponding author: Wen Zhou, School of Energy and Environment, City University of Hong Kong, Hong Kong, China, 2/F Harbour View 2, 16 Science Park East Avenue, Hong Kong Science Park Shatin, N.T., Hong Kong, China
E-mail: wenzhou@cityu.edu.hk

on dry/wet conditions over Japan, China, and the United States during summer season (June-August) and suggested that different tropical Pacific SST variations between El Niño Modoki and El Niño events may be related to different teleconnections and climate impacts on summer rainfall in the Pacific Rim. Ashok and Yamagata (2009) suggested that anthropogenic warming might accelerate shifts in El Niño phenomena. More importantly, it appears that the El Niño Modoki have increased in frequency in the recent years (Ashok et al. 2007; Pradhan 2011) and the future climate state will be favorable for more frequent and intense El Niño Modoki events under global warming (Yeh et al. 2009; Lee and McPhaden 2010; Na et al. 2011). However, observational studies are largely limited by sample size, and it remains an open question if the recent trends in El Niño Modoki are indicative of a climate change signal (Newman et al. 2011). Nonetheless, from the standpoint of understanding the regional impacts related to precipitation, what is particularly salient is that this nuanced view of Pacific sea surface temperature variability is likely to provide twofold knowledge: (1) regional patterns of precipitation sensitivity to El Niño Modoki and (2) a clearer perspective regarding the potential future impacts, contingent upon changing statistics of El Niño Modoki.

The purpose of the present study is to explore the relative impacts of the two types of El Niño: Canonical El Niño and El Niño Modoki on precipitation over the Korean peninsula. Since the impact of El Niño on rainfall is more significant after the mature phase of El Niño (Feng et al. 2010; Zeng et al. 2011), our work is focused mainly on the decaying years of the El Niño and El Niño Modoki. In the following sections, we describe the data and research methodology used in this study (Section 2), followed by discussion of the spatial variability in the magnitude and frequency of summer precipitation for the five major Korean river basins and their sub-watersheds under different ENSO conditions (Section 3). The main features of the associated large-scale atmosphere circulations are described in Section 4. Finally, the summary and conclusions are reported in Section 5.

2. Data and Methods

The analysis presented here is based on spatially averaged daily precipitation provided by the Korean Water Resources Management Information System (WAMIS 2011; http://www.wamis.go.kr/) during the 1966–2007 period. The network density of precipitation gauges often causes errors in the spatial interpolation of areal averages. However, precipitation stations (Han River Basin 43, Nakdong River Basin 45, Geum River Basin 28, Sumjin River Basin 17, and Yeongsan River Basin 7) are relatively well distributed over South Korea (Kim and Jain 2011). The atmospheric data (1965–2007) are obtained from the National Centers for Environmental Prediction-National Center for Atmospheric Research (NCEP-NCAR) reanalysis (Kistler et al. 2001). The geopotential height anomalies at 850-hPa and integrated moisture flux, obtained from the surface to 700-hPa, were used for the composite analysis. To understand the empirical relationship between warm–season precipitation at the watershed scale and large-scale climate, we defined strong ENSO warm events based on the Niño-3 index and El Niño Modoki index (EMI) suggested by Ashok et al. (2007). In this study, the El Niño events are identified by the normalized 3-month moving average Niño-3 index exceeding the upper quartile (0.45) and persisting for 8 months from June to February. El Niño Modoki events are defined by the normalized 3-month moving average EMI exceeding the upper quartile (0.66) and persisting for 6 months from September to February. Based on these two criteria, the six strongest El Niño events (1969/70, 1972/73, 1976/77, 1982/83, 1987/88, 1997/98) and the eight strongest El Niño Modoki events (1967/68, 1977/78, 1986/87, 1990/91, 1991/92, 1994/95, 2002/03, 2004/05) are chosen from 1966 to 2007. However, based on SST anomaly patterns in 1969/70 (Appendix Fig. 1), it is found that in addition to the warming in the eastern tropical Pacific, another warming center is observed west of 150°W, which is similar to the El Niño Modoki warming condition. The impact of the 1997/98 El Niño event is clearly distinct from the other events, which must be discussed individually (Appendix Fig. 1). To clearly compare the influences of the two kinds of El Niño, the 1969/70 and 1997/98 El Niño events are not selected. Compared to the other El Niño Modoki events, the warming center during the 1991/92 is located in the eastern Pacific Ocean, with the most warming observed to the east of 150°W (Appendix Fig. 2); thus this case is also excluded. Consequently, we have used only four decaying El Niño years (1973, 1977, 1983, and 1988) and seven decaying El Niño Modoki years (1968, 1978, 1987, 1991, 1995, 2003, and 2005) for the composite analysis in this study. Composite analysis is conducted mainly to identify the impacts of the two different phases of El Niño on dry and wet conditions in South Korea. The statistical significance test for the composite analysis is performed using Monte Carlo resampling techniques.

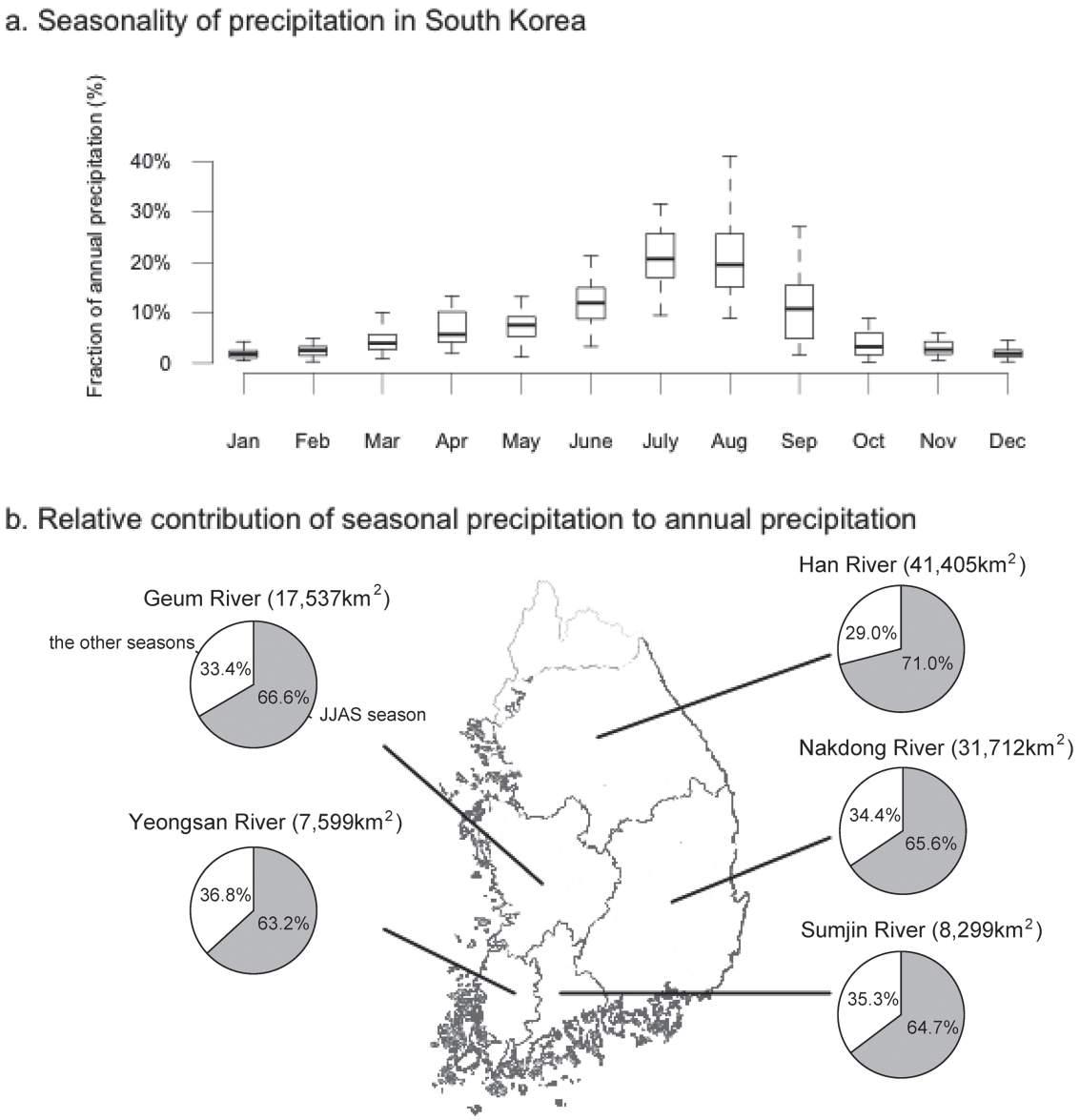

Fig. 1. Seasonality of precipitation in South Korea from 1966–2007. a. Fraction of annual total precipitation. For each month, rainfall variability is summarized using a boxplot (0, 0.25, 0.5, 0.75, 1.0 quantile levels are shown). b. Seasonal fraction of annual precipitation for five major river basins in Korea. In the pie chart, the fraction of annual precipitation occurring in the summer season (JJAS) is highlighted with gray shading.

3. Analysis and Results

3.1 Precipitation variability related to El Niño and El Niño Modoki phases

Approximately 68% of the total annual precipitation in South Korea occurs during the summer season (June-September**;** Fig. 1). The highest contribution of seasonal precipitation to annual precipitation is seen in the Han River Basin (873 mm, 71% of the annual totals). The remaining regions have less precipitation, but account for more than two-thirds of the annual precipitation. The range in seasonal precipitation in five major river basins is from 821 mm to 934 mm. During this warm season, seasonal precipitation and extremes are critically important for water supplies for both human and environmental needs (Postel and

Richter 2003; Poff et al. 2010; Kim and Jain 2011; Kim et al. 2011b).

Dynamic variations in the East Asian monsoon and tropical cyclones in the western North Pacific (WNP) have modest potentials to increase our understanding of the variations in seasonal precipitation and extremes in South Korea. However, recent studies (Ashok et al. 2007; Weng et al. 2007; Taschetto and England 2009; Yeh et al. 2009) that characterize central tropical Pacific warming (often referred to as El Niño Modoki) and its teleconnections to the East Asia show coherent teleconnection patterns during boreal summer. In the following sections, therefore, we pursue an exploratory analysis to improve understanding of the potential impacts of the new type of El Niño on seasonal precipitation totals, maximum precipitation, and extreme rainy days for Korea's five major river basins.

a. Seasonal precipitation totals

Figure 2 shows the empirical probability distribution of seasonal precipitation in the five major river basins (Han River, Nakdong River, Geum River, Sumjin River, and Yeongsan River) during decaying phases of the selected El Niño and El Niño Modoki. Here, seasonal rainfall totals are standardized by the long-term mean and standard deviation of rainfall (1971–2000). The patterns of precipitation anomalies indicate significant difference between El Niño and El Niño Modoki. For the El Niño years, the probability density functions (PDF) display sharp distributions and positive skew for all basins, indicating that negative anomalies are generally found. In contrast, for the El Niño Modoki years, the conditional distributions clearly show positive anomalies in seasonal precipitation. Distinct positive anomalies appear in the Han and Geum river basins. Figure 3 compares the composite precipitation anomalies (shown as a percentage to normal) during the June-September season. The largest contrasts in precipitation anomalies are also seen in the Han and Geum river basins. During El Niño Modoki, 16 out of 29 sub-basins (49.6% of the total area) in the Han River Basin show significant above-normal precipitation. In the Geum River Basin, 11 out of 21 sub-basins, which account for 62.4% of the total area, exhibit significantly wet conditions. In the remaining basins, there are no significant changes in warm-season precipitation, except 1 sub-basin in the Nakdong River Basin. During El Niño, significant suppressed precipitation occurs over the Korean peninsula (Han River Basin: 100% of the total area, Nadong River Basin: 84.6% of the total area, Geum River Basin: 99.3% of the total area, Sumjin River Basin: 100% of the total area, Yeongsan River Basin: 100% of the total area). Consequently, significant dry conditions are experienced over South Korea during El Niño. In contrast, the distinct wet signals occur in the central Korean peninsula (29.8% of the total area of South Korea) in the decaying years of the selected El Niño Modoki events. The spatial patterns of variations in seasonal precipitation totals vary by event. Therefore, we construct the sea surface temperature (SST) and the precipitation anomalies during each decaying phase of the selected El Niño and El Niño Modoki (refer to figures in the appendix).

b. Extreme precipitation events

Extreme weather or climate episodes play a critical role in altering hydrologic regimes in riverine and riparian processes, such as high sediment loads and redistribution processes in streams (Poff and Ward 1990; Mathews and Richter 2007). In South Korea, extreme precipitation events, which are mainly related to the East Asian summer monsoon (also referred to as the Meiyu-Baiu front or Changma front) and tropical cyclones, occurred during the June-September season (Kim et al. 2011a, b). Figure 4 shows composite anomalies of seasonal maximum precipitation during El Niño and El Niño Modoki years. For the El Niño years, below-normal peaks are found over the Korean peninsula (Fig. 4a). The most significant changes are seen in the Sumjin River Basin (13 out of 15 sub-basins, 92.1% of the total area), followed by the Yeongsan River Basin (13 out of 15 sub-basins, 90.6% of the total area), Geum River Basin (9 out of 21 sub-basins, 72.5% of the total area). The Han and Nakdong river basins show relatively less significant results of 55.9% and 51.6% of the total area, respectively. In contrast, for the El Niño Modoki years, significant increases in extreme precipitation events are widespread over the Geum and Nakdong river basins and some regions in the Han River Basin (Fig. 4b). The most significant positive anomalies are found in the Geum River Basin (52.0% of total area). Along the east coast and some parts in the Nakdong River Basin, statistically significant positive anomalies are seen (16 out of 33 sub-basins, 38.3% of the total areas). In the Han River Basin, 8.0% of the total areas (4 out of 29 sub-basins) show significant change in seasonal maximum precipitation.

c. Frequency of heavy precipitation events

The significant increasing trends in the number of heavy-rain days (≥30 mm/day and ≥50 mm/day) are fairly widespread over the Korean peninsula (Chang and Kwon 2007, Kim and Jain 2011). Figure 5 shows

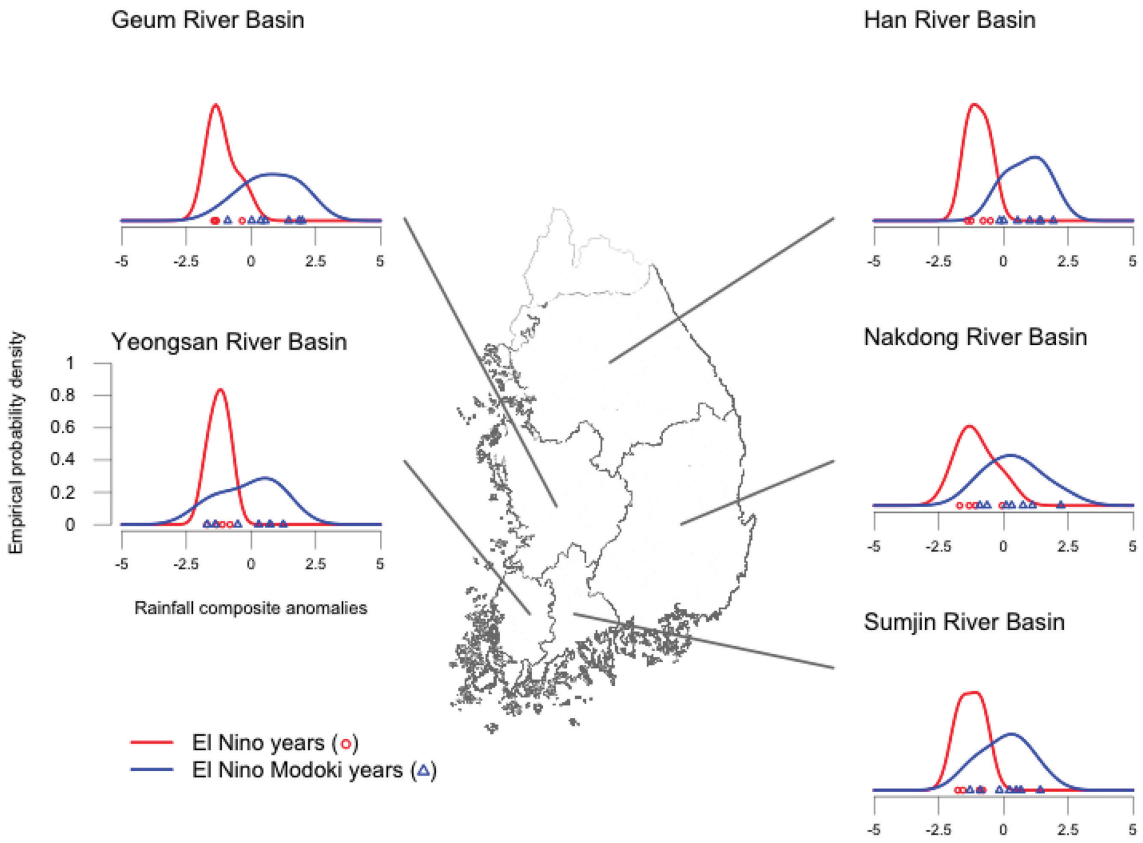

Fig. 2. Empirical probability density function for the seasonal rainfall composite anomalies (June-September) for the five major river basins in South Korea. The red line indicates the distribution of seasonal rainfall anomalies during the canonical El Niño. The blue line shows precipitation variability during ENSO Modoki events. In each figure, symbols on the bottom line represent rainfall anomalies corresponding to El Niño years (red circles) and ENSO Modoki years (blue triangles)

the composite results of the frequency of heavy precipitation events, which are similar to those shown in Fig. 3. This is not surprising, because the number of heavy-rain days is highly correlated with the seasonal precipitation total (Kim and Jain 2011). For the El Niño years (Figs. 5a, c), the significant negative anomalies in the frequency of heavy precipitation (≥30 mm/day) appear widespread over South Korea (Fig. 5a). Significant dry conditions are shown in areas in the Yeongsan River Basin (14 out of 14 sub-basins), Geum River Basin (20 out of 21 sub-basins), Sumjin River Basin (14 out of 15 sub-basins), and Han River Basin (25 out of 29 sub-basins). In the Nakdong River Basin, 25 out of 33 sub-basins show fewer wet days. The anomalies with heavy-rain days (≥50 mm/day) shown in Fig. 5c represent basically similar patterns to anomalies with rainy days (≥30 mm/day). For the El Niño Modoki years (Figs. 5b, d), the distinct changes in heavy-rain days are detected mostly in the Han and Geum river basins. The distributions of composite anomalies with heavy precipitation (≥30 mm/day) are as follows (Fig. 5b): Geum River (57.9% of the total area), Han River (44.3% of the total area), Sumjin River (13.7% of the total area), and Nakdong River Basin (10.0% of the total area). The Yeongsan River Basin shows no significant changes. For the anomalies with heavy-rain days (≥50 mm/day) shown in Fig. 5d, 20 out of 29 sub-basins in the Han River Basin (55.1% of the total area) experience significant changes along the eastern coastal and central part of the region. In the Geum River Basin, 9 out of 21 sub-basins (42.1% of the total area) show significant extreme wet days. The large-scale atmospheric circulation is responsible for the precipitation changes. In the next section, we

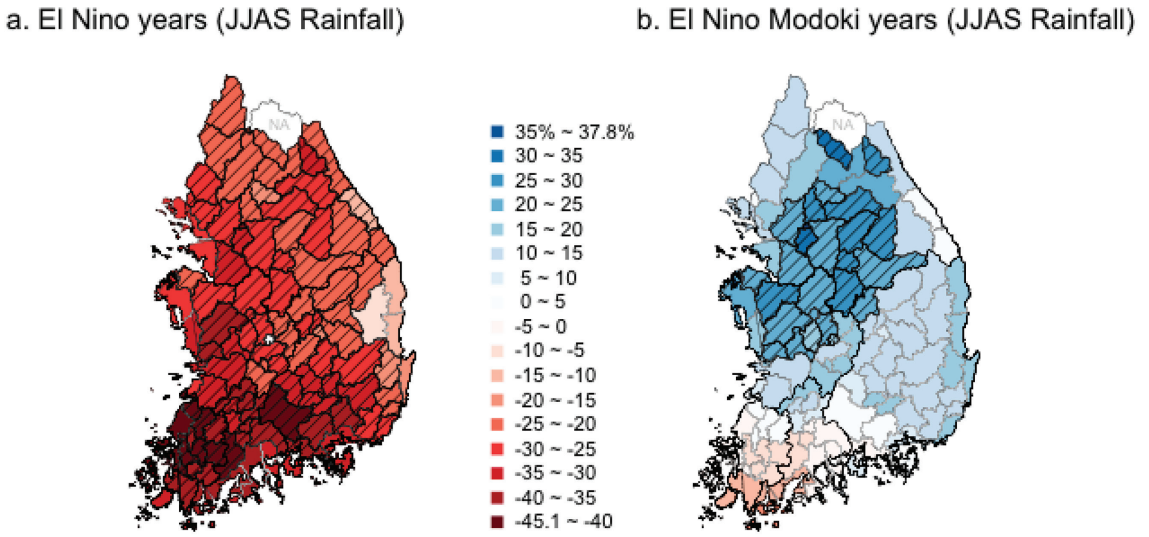

Fig. 3. Percentage change in composite anomalies of seasonal rainfall (departures from 1971–2000 norms) during (a) El Niño years and (b) El Niño Modoki years over the Korean Peninsula. The effects of both phases of ENSO are shown with different color schemes (increases in blues and decreases in reds). The hatched polygons show statistically significant changes in seasonal precipitation totals (June-September) based on a 90% confidence level. Note: NA means no data is available.

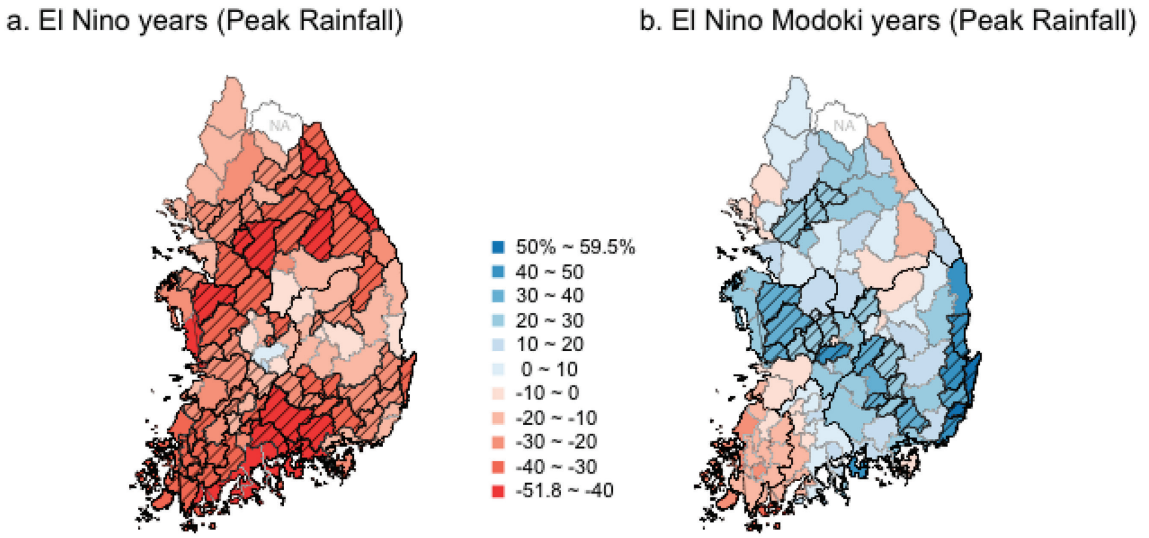

Fig. 4. Percentage changes in composite anomalies of seasonal maximum rainfall (departures from the 1971–2000 norms) during (a) El Niño years and (b) El Niño Modoki years over the Korean Peninsula. The effects of both phases of ENSO are shown with different color schemes (increases in blues and decreases in reds). The hatched polygons show statistically significant changes in seasonal maximum rainfall (June-September) based on a 90% confidence level. Note: NA means no data is available.

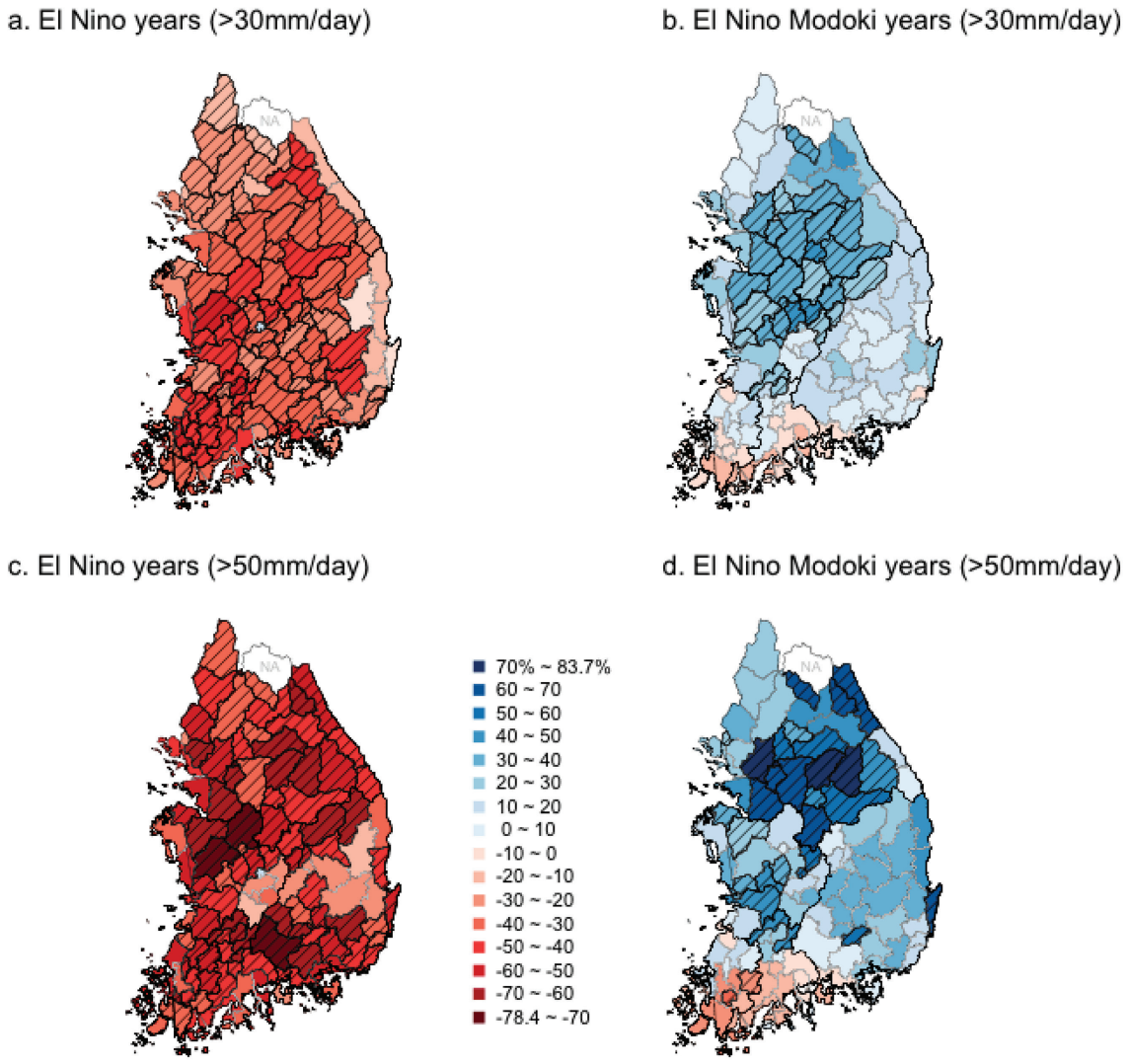

Fig. 5. Percentage changes in composite anomalies (departures from 1971–2000 norms) of the number of rainy days with heavy precipitation (≥30mm/day and ≥50mm/day) corresponding to both phases of El Niño and El Niño Modoki over the Korean Peninsula. The effects of both phases of ENSO are shown with different color schemes (increases in blues and decreases in reds). The hatched polygons show statistically significant changes in heavy-rain days (≥30mm/day and ≥50mm/day) during the June-September period based on a 90% confidence level. Note: NA means no data is available.

discuss some of the teleconnection patterns associated with El Niño and El Niño Modoki that are most likely to induce both wet and dry conditions.

3.2 Large-scale atmospheric circulations associated with El Niño and El Niño Modoki

The ENSO teleconnection impacts on climate changes over East Asia have been well documented by many researchers (Chang et al. 2000; Wang et al. 2000; Chan and Zhou 2005; Li et al. 2006; Zhou et al. 2007a, b; Wang et al. 2011). Furthermore, it has been recognized that ENSO has an important influence on the East Asian monsoon during the summer time (Chan and Zhou 2005; Zhou and Chan 2007; Zhou et al. 2009). Recently, El Niño Modoki has been identified as a new type of El Niño in the central Pacific (Ashok et al. 2007; Weng et al. 2007; Feng et al. 2010). There has been a renewed interest in the El Niño Modoki phenomenon,

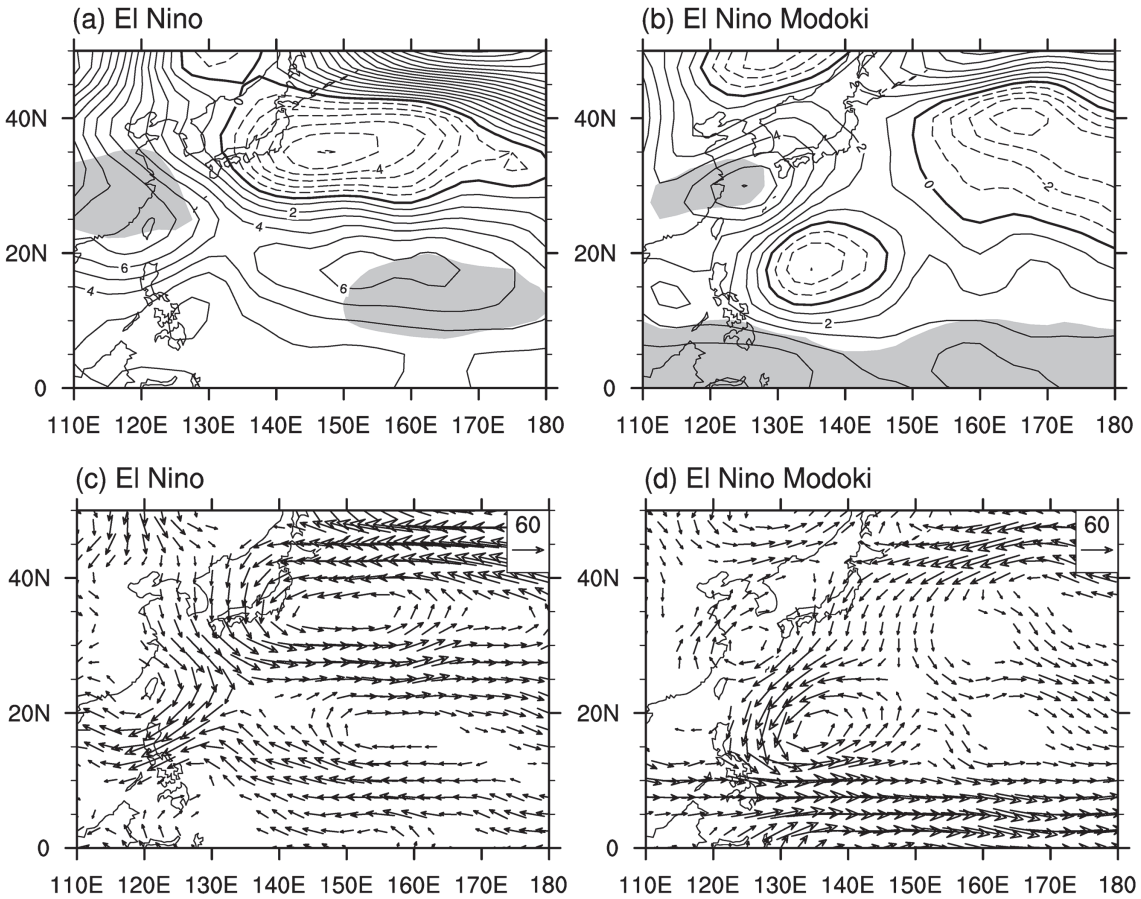

Fig. 6. Composite differences of JJAS geopotential height anomalies at 850-hPa (upper panels) and vertically integrated (1000–700hPa) water vapor flux (unit: kg/m/s, lower panels) of El Niño (a and c) and El Niño Modoki (b and d) decaying phases with La Niña. The La Nina events are 1971, 1974, 1976, 1989, 1999, and 2000. The shading in (a) and (b) represents anomalies exceeding the 90% significance level. The magnitude of the vectors exceeding 15 kg/m/s is plotted in (c) and (d).

especially among many countries bordering the Pacific Ocean.

Atmospheric moisture transport could have potential implications for the regional variability in precipitation. Figure 6 presents the composite geopotential height anomalies at 850-hPa and the vertically integrated (1000-700-hpa) moisture fluxes. In the summer of the decaying year of the El Niño, the anomalous Philippine Sea anticyclone is seen in the lower troposphere (Fig. 6a) consistent with previous studies and is a Rossby-wave response to the in situ ocean surface cooling and the subsidence forced remotely by the El Niño warming (Wang et al. 2000). This result indicates that the western North Pacific subtropical high has retreated southeastward to south of 30°N. At mid-latitude, there is an anomalous low center to the east of Japan. Under the control of these large-scale circulation patterns, dry air from high-latitudes is transported to South Korea during El Niño, which results in less wet-season rainfall (Fig. 6c). In contrast, for El Niño Modoki (Fig. 6b), the positive anomalies are over eastern China, the Korean peninsula and Japan, and the significant high is located over mid-eastern China and southern Korea accompanied by the geopotential height anomalies of the opposite sign to the north and southeast. An anomalous cyclone locates east of the Philippines, which clearly reflects the Gill's (Gill 1980; Lee et al. 2009; Wang et al. 2010) response to the warm SST anomalies in the equatorial central Pacific. Based on the dynamics theory of Gill (1980)

that the equatorial warm SST anomalies can produce cyclone anomalies in the northwest of heating region, the cyclone anomalies tend to be expected as a westward shift of the tropical Pacific warm during El Niño Modoki. The local contributions of the tropical western North Pacific SST anomalies on these cyclone and anticyclone circulation anomalies need further studies. The patterns with anomalous high and anomalous low over the western North Pacific is referred as a positive phase of the Pacific-Japan pattern (Nitta 1987), indicating that the western North Pacific subtropical high intensifies and shifts northwestward (130°E, 30°N) from its climatological mean. The negative anomalies to the north of Japan and Korea imply that the Okhotsk high is unusually weak. The position and intensity of these anomaly centers clearly allow low-level moisture to be conveyed to South Korea from the western North Pacific during El Niño Modoki (Fig. 6d), which favors more precipitation over South Korea. Consequently, the large-scale atmospheric circulations over East Asia and the western North Pacific related to the two types of El Niño in their decaying phases are totally different, which is consistent with previous results (Weng et al. 2007; Feng et al. 2011). The resulting moisture flux patterns could lead to different precipitation changes over the Korean peninsula.

4. Summary and Conclusions

This study pursued an exploratory analysis of regional precipitation patterns over the Korean peninsula within the context of two different types of El Niño. The results show distinct spatial precipitation anomaly patterns related to El Niño and El Niño Modoki. The main impacts of the two types of El Niño on summer precipitation for Korea's five major river basins can be summarized as follows:

1. During the El Niño years, significant drier conditions are observed throughout South Korea. In contrast, in the El Niño Modoki years, wetter conditions prevail over the interior and western river basins, especially the Geum (62.4 %) and the Han (49.6%).

2. For extreme precipitation events, the largest contrast of precipitation anomalies is seen in the Geum River Basin (negative anomalies in El Niño years: 72.5%, positive anomalies in El Niño Modoki years: 52.0%), followed by the Nakdong River Basin (negative anomalies in El Niño years: 51.6%, positive anomalies in El Niño Modoki years: 38.3%). The extreme precipitation event may also cause significant changes in riverine and riparian processes of erosion or deposition of sediment, which have a critical impact on habitat for many species.

3. The significant negative anomalies in the frequency of heavy precipitation (≥30 mm/day and ≥50 mm/day) are widespread over South Korea in the El Niño years. During the El Niño Modoki years, the most significant positive changes in the number of heavy-rain days are observed mainly in the Geum River Basin (≥30 mm/day: 57.9%, ≥50 mm/day: 42.1%) and the Han River Basin (≥30 mm/day: 44.3%, ≥50 mm/day: 55.1%).

In this study, we confirm that El Niño and El Niño Modoki events produce strikingly different precipitation anomaly patterns in South Korea during the warm season. Through the different atmospheric teleconnections over East Asia and the western North Pacific, the SST warming patterns over the tropical Pacific during El Niño and El Niño Modoki induce changes in water vapor flux over South Korea, resulting in precipitation pattern differences. It is also important to note that the results presented here are limited by the small number of historical observations, and thus should be regarded as illustrative rather than definitive. However, we expect the present analysis to provide improved understanding of the potential impacts of the tropical Pacific sea surface temperature on warm-season water availability and hydrometeorological extremes over the Korean peninsula.

Acknowledgments

The authors would like to express the gratitude for valuable comments provided by two anonymous reviewers. The work described in this paper was supported by National Nature Science foundation of China Grant 4117507 and CityU Strategic Research Grant 7002717.

References

Ashok, K., S. Behera, S. Rao, H. Weng, and T. Yamagata, 2007: El Niño Modoki and its possible teleconnection. *J. Geophys. Res.,* **112**, C11007, doi:10.1029/2006/JC003798.

Ashok, K., and T. Yamagata, 2009: The El Niño with a difference. *Nature*, **461**, 481–484.

Chan, J. C. L., and W. Zhou, 2005: PDO, ENSO and the summer monsoon rainfall over South China. *Geophys. Res. Lett.,* **32**, L08810.

Chang, C. P., Y. Zhang, and T. Li, 2000: Interannual and interdecadal variations of the East Asian summer monsoon and tropical Pacific SSTs. Part I: Roles of the subtropical ridge. *J. Climate.,* **13**, 4310–4325.

Chang, H. J., and W. T. Kwon, 2007: Spatial variations of summer precipitation trends in South Korea 1973–2005. *Environ. Res. Lett*., **2**, 045012.

Feng, J., W. Chen, C. Y. Tam, and W. Zhou, 2010: Different impacts of El Niño and El Niño Modoki on China

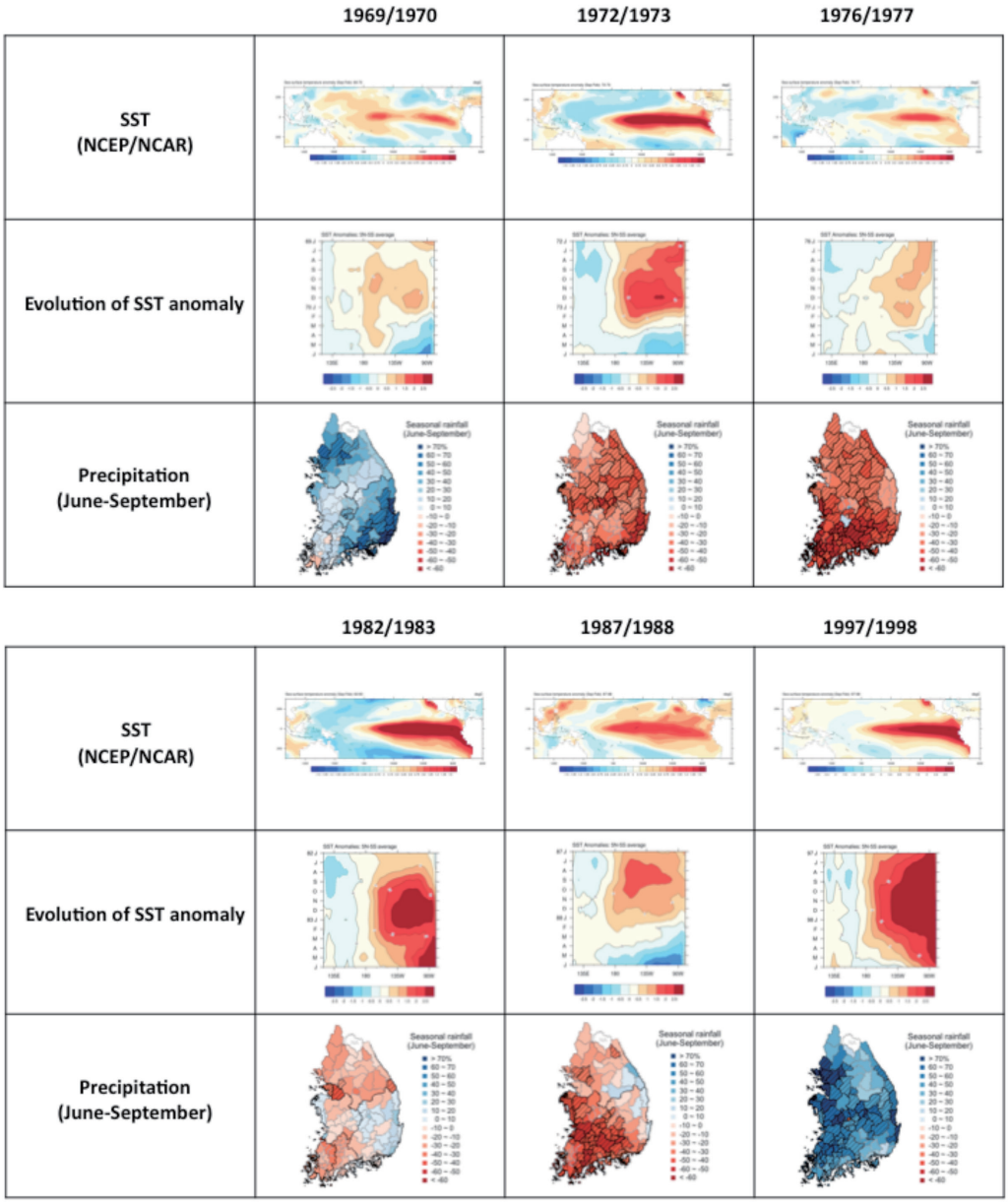

Appendix. 1. SST anomalies for the El Niño events. SST anomaly patterns during each El Niño in developing, peak phases, and precipitation over South Korea corresponding to the El Niño decaying phase.

rainfall in the decaying phases. *Int. J. Climatol.,* doi: 10.1002/joc.2217.

Gill, A. E., 1980: Some simple solutions for heat-induced tropical circulation. *Quart. J. Roy. Meteor. Soc.*, **106**, 447–462.

Kao, H. Y., and J. Y. Yu, 2009: Contrasting eastern-Pacific and central-Pacific types of ENSO. *J. Climate,* **22**, 615–632, doi: 10.1175/2008JCLI2309.1.

Kim, J. S., and S. Jain, 2011: Precipitation trends over the Korean peninsula: typhoon-induced changes and a typology for characterizing climate-related risk *Environ. Res. Lett.*, **6**, 034033, doi:10.1088/1748–9326/6/3/034033.

Kim, J. S., S. Jain, and S.K. Yoon, 2011a: Warm season streamflow variability in the Korean han River Basin: Links with atmospheric teleconnections. *Int. J.*

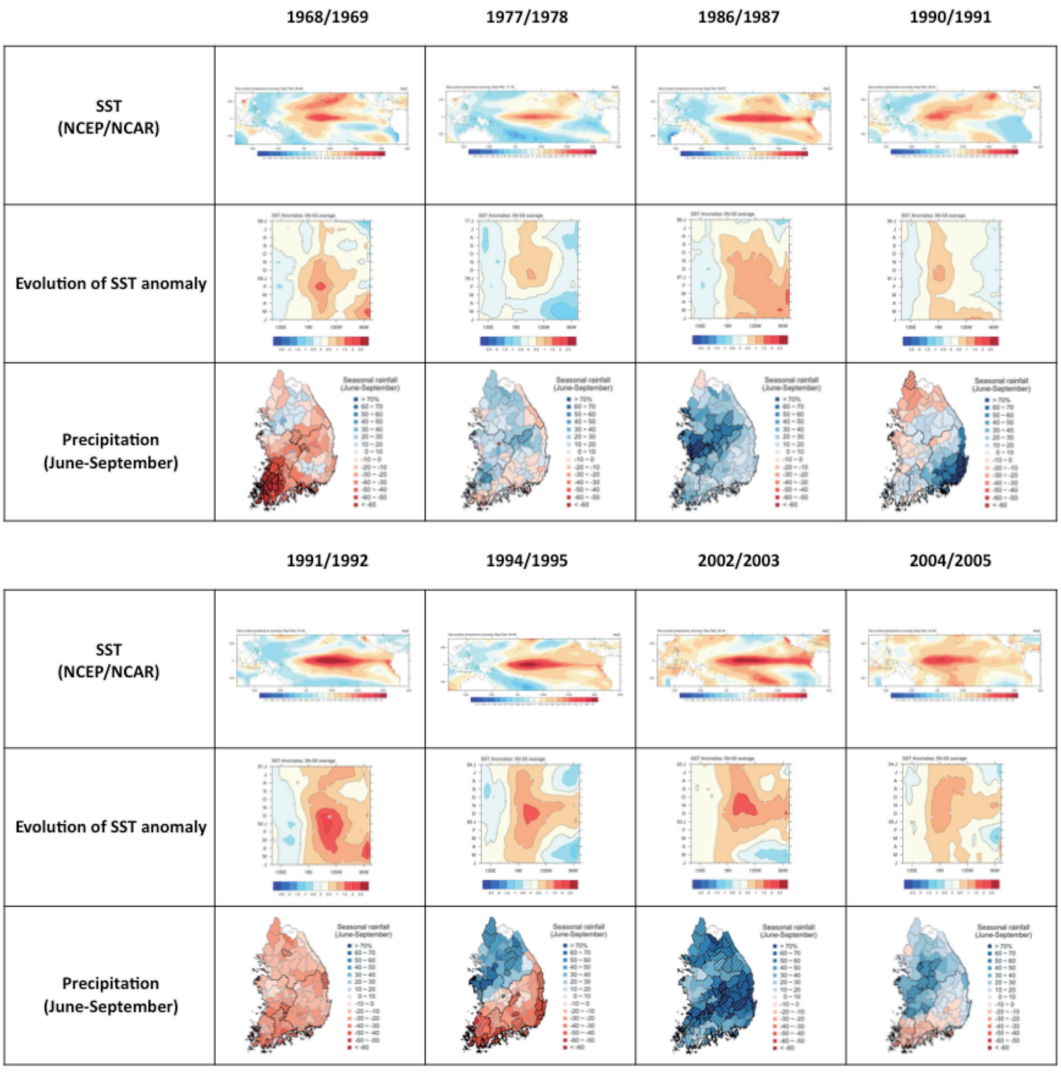

Appendix. 2. SST anomalies for the El Niño Modoki events. SST anomaly patterns during each El Niño Modoki in developing, peak phases, and precipitation over South Korea corresponding to the El Niño Modoki decaying phase.

Climatol., **32**, 635–640.

Kim, J. S., S. Jain, and Y. I. Moon, 2011b: Atmospheric teleconnection-based conditional streamflow distributions for the Han River and its sub-watersheds in Korea. *Int. J. Climatol.,* doi:10.1002/joc.2374.

Kistler, R., and Coauthors, 2001: The NCEP–NCAR 50-year reanalysis: Monthly means CD-ROM and documentation. *Bull. Amer. Meteor. Soc.,* **82**, 247–267.

Kug, J. S., F. F. Jin, and S. I. An, 2009: Two types of El Niño events: Cold tongue El Niño and warm pool El Niño. *J. Climate.,* **22**, 1499-1515, doi:10.1175/2008JCLI2624.1.

Lee, S. K., C. Wang, and B. Mapes, 2009: A simple atmospheric model of the local and teleconnection response to heating anomalies. *J. Climate*, **22**, 272–284.

Lee, T., and M. J. Mc Phaden, 2010: Increasing intensity of El Niño in the central-equatorial Pacific. *Geophys. Res. Lett*., **37**, L14603, doi:10.1029/2010GL044007.

Li, C. Y., W. Zhou, X. L. Jia, and X. Wang, 2006: Decadal/interdecadal variations of ocean temperature and its impacts on climate. *Adv. Atmos. Sci.,* **23**, 964-981.

Mathews, R., and B. D. Richter, 2007: Application of the indicators of hydrologic alteration software in environmental flow setting. *J. Am. Water Resour. As.*, **43**, 1400–1413.

Na, H., B. G. Jang, W. M. Choi, and K. Y. Kim, 2011: Statis-

tical simulations of the future 50-year statistics of cold-tongue El Niño and warm-pool El Niño. *Asia-Pacific J. Atmos. Sci.*, **47**, 223–233.

Nitta, T., 1987: Convective activities in the tropical western Pacific and their impact on the Northern Hemisphere summer circulation. *J. Meteor. Soc. Japan.,* **65**, 373–390.

Poff, N. L., and J. V. Ward, 1990: Physical habitat template of lotic systems-Recovery in the context of historical pattern of spatio-temporal heterogeneity. *Environ. Manage.,* **14**, 629–645.

Poff, N. L., and others, 2010: The ecological limits of hydrologic alteration (ELOHA): A new framework for developing regional environmental flow standards. *Freshwater Biology*, **55**, 147–170.

Postel, S., and B. Richter, 2003: Rivers for Life: Managing Water for People and Nature Island. Press:Washington DC USA.

Pradhan, P. K., B. Preethi, K. Ashok, R. Krishna, and A. K. Sahai, 2011: Modoki, Indican Ocean dipole, and western North Pacific typhoons: Possible implications for extreme events. *J. Geophys. Res.*, **116**, D18108, doi: 10.1029/2011JD015666.

Ren, H. L., and F. F. Jin, 2011: Niño indices for two types of ENSO. *Geophys. Res. Lett.*, **38**, L04704, doi: 10.1029/2010GL046031.

Taschetto, A. S., and M. H. England, 2009: El Niño Modoki impacts on Australian rainfall. *J. Climate*, **22**, 3167–3174.

WAMIS (Water Management Information System), 2011: http://wamis.go.kr/eng/ accessed 8 November 2011

Wang, B., R. Wu, and X. Fu, 2000: Pacific–East Asian teleconnection: How does ENSO affect East Asian climate? *J. Climate*, **13**, 1517–1536.

Wang, B., and Q. Zhang, 2002: Pacific-East Asian teleconnection. Part II: How the Philippine Sea anomalous anticyclone is established during El Niño development. *J. Climate,* **15**, 3252–3265.

Wang, C., S. K. Lee, and C. R. Mechoso, 2010: Interhemispheric influence of the Atlantic warm pool on the southeastern Pacific. *J. Climate*, **23**, 404–418.

Wang, X., D. Wang, and W. Zhou, 2009: Decadal variability of twentieth century El Niño and La Niña occurrence from observations and IPCC AR4 coupled models. *Geophys. Res. Lett.,* **36**, L11701, doi: 10.1029/2009GL037929.

Wang, X., D. Wang, W. Zhou, and C. Y. Li, 2011: Interdecadal modulation of the influence of La Niña events on mei-yu rainfall over the Yangtze River Valley. *Adv. Atmos. Sci.*, **29**, doi: 10. 1007/s00376-011-1021-8.

Weng, H. Y., K. Ashok, S. K. Behera, S. A. Rao, and T. Yamagata, 2007: Impacts of recent El Niño Modoki on dry/wet conditions in the Pacific rim during boreal summer. *Clim. Dyn.*, doi: 10.1007/s00382-007-0234-0.

Yeh, S. W., J. S. Kug, B. Dewitte, M. H. Kwon, B. P. Kirtman, and F. F. Jin, 2009: El Niño in a changing climate. *Nature*, **461**, 511–514, doi:10.1038/nature08316.

Zeng, X. F., B. Li, L. Feng, X. J. Liu, and T. J. Zhou, 2011: East China Summer Rainfall during ENSO Decaying Years Simulated by a Regional Climate Model, *Atmos. Oceanic. Sci. Lett.*, **4**, 91–97.

Zhou, W., C. Li, and X. Wang, 2007a: Possible connection between Pacific oceanic interdecadal pathway and East Asian winter monsoon. *Geophys. Res. Lett.,* **34**, L01701, doi: 10.1029/2006GL027809.

Zhou, W., X. Wang, T. J. Zhou, C. Y. Li, and J. C. L. Chan, 2007b: Interdecadal variability of the relationship between the East Asian winter monsoon and ENSO. *Meteorol Atmos. Phys.* **98,** 283–293, doi: 10.1007/s00703-007-0263-6.